Desalination and Water Treatment
www.deswater.com
doi: 10.5004/dwt.2020.25472

191 (2020) 231–238
July

Adsorption removal of pharmaceutical and personal care products with functionalized metal-organic framework: adsorptive selectivity and mechanism

Wan Zhou, Qizhou Dai, Tingting Zhan, Lin Wang, Xinze Bian, Siqi Fan, Pan Xiong, Yi Xia, Jianmeng Chen*

College of Environment, Zhejiang University of Technology, Hangzhou 310032, China, Tel./Fax: +86-571-88320276; emails: jchen@zjut.edu.cn (J. Chen), 316170058@qq.com (W. Zhou), dqz@zjut.edu.cn (Q. Dai), 2712443661@qq.com (T. Zhan), 1414695278@qq.com (L. Wang), 1225093188@qq.com (X. Bian), 2401945777@qq.com (S. Fan), 1150628076@qq.com (P. Xiong), 603510916@qq.com (Y. Xia)

Received 9 June 2019; Accepted 14 January 2020

ABSTRACT

Pharmaceutical and personal care products (PPCPs) had been detected worldwide as an emerging contaminant in the aquatic system. Herein, we reported a kind of NH_2-functionalized UiO-66 which exhibited effective removal toward diflunisal and salicylic acid. The capacity of UiO-66-NH_2 was much higher than commercial activated carbon (AC) for the adsorption of PPCPs and it was because UiO-66-NH_2 had a smaller pore size than AC. The UiO-66-NH_2 also indicated some interactions, like π–π stacking and electrostatic interaction. The removal efficiency of diflunisal and salicylic acid from wastewater with the UiO-66-NH_2 groups was higher than the original UiO-66. It could be explained with the acid-base attraction between the NH_2 group of UiO-66-NH_2 and the COOH group of diflunisal and salicylic acid. However, the performance of UiO-66-NH_2 in the adsorption of carbamazepine was not very desirable. The base–base repulsion between the NH_2 group of UiO-66-NH_2 and the NH_2 group of carbamazepine led to a decrease in the adsorption capacity of UiO-66-NH_2. The UiO-66-NH_2 could be regenerated with ethanol and reused for the adsorption removal of the adsorbates.

Keywords: Adsorption; Metal-organic frameworks; UiO-66; Acid-base attraction; Pharmaceutical and personal care products

1. Introduction

Due to the growth of the world population and rapid urbanization, pharmaceutical, and personal care products (PPCPs) were increasingly popular in our daily life, such as prescription medicines and sunscreens, etc. [1,2]. Numerous PPCPs, like diflunisal, were discharged into the environment and could be found in surface water [3]. The accumulation of PPCPs caused water pollution, which was harmful to the environment of aquatic organisms [4,5]. The removal of these PPCPs from the water was valued by researchers all over the world.

Various technologies, such as coagulation and flocculation [6], biodegradation [7,8], ultrasonic treatment [9], electrochemical oxidation [10–13], and ozonation [14–16], had been applied to remove PPCPs in aqueous solution. The adsorption technology was also widely used to remove PPCPs due to its simple process, low energy consumption, and few by-products [17]. The most widely used adsorbent was commercial activated carbon (AC) [18].

Over the past two decades, kinds of novel materials had been received increasing attention for the application of environmental protection and energy conversion [19,20]. Metal-organic frameworks (MOFs) showed huge potential

* Corresponding author.

in adsorption. It was a novel porous crystal material with a self-assembled metal center and an organic ligand. Moreover, it had a three-dimensional network ordered pore structure with ultra-high specific surface area, species and structure diversity, and chemical function [21]. Based on these excellent properties, MOFs had become a research hotspot in the field of new porous materials. They had potential for adsorbent [22,23], catalyst [24], and membrane materials [25,26]. The Cavka research group at the University of Oslo, Norway, firstly reported a kind of Zr-based metal-organic framework which was called UiO-66 [27]. It was widely used because of its excellent hydrothermal stability, high porosity, and easy functionalization [28].

In this research, UiO-66 and UiO-66-NH_2 were used to remove diflunisal, salicylic acid (2-Hydroxybenzoic acid; CAS# 69-72-7), and carbamazepine (5H-Dibenzo [b, f] azepine-5-carboxamide; CAS# 298-46-4) from water. Both adsorbates and UiO-66 contained benzene rings and they had probable interactions, such as π–π interactions between adsorbates and UiO-66. These interactions were beneficial for adsorption removal. All adsorbates were also removed with UiO-66-NH_2. A plausible adsorption mechanism based on acid-base interactions was suggested between the adsorbates and UiO-66-NH_2. In addition, the adsorption isotherms and adsorption kinetics were also studied. The following regeneration by ethanol washing, the reusability of UiO-66-NH_2 could be confirmed by several simple cycle experiments.

2. Materials and methods

2.1. Materials

All the chemicals were obtained from commercial vendors without further purification. Zirconium chloride ($ZrCl_4$, 98%), terephthalic acid (H_2BDC, 99%), amino-terephthalic acid (NH_2-BDC, 99%), diflunisal (98%), salicylic acid (98%), and carbamazepine (98%) were obtained from Sigma-Aldrich (Shanghai, China). Amino-terephthalic acid (NH_2-BDC, 98%) was purchased from Macklin (Shanghai, China). N, N-Dimethylformamide (DMF, 99.5%), methanol (99.5%), ethanol (95%), and acetic acid (CH_3COOH, 99.5%) were obtained from Shanghai Lingfeng Chemical Reagent Co., Ltd., (Shanghai, China). Hydrochloric acid (HCl, 36–38%), Sodium hydroxide (NaOH, 96%) were purchased from Xilong Scientific Co., Ltd., (Shantou, China).

2.2. Synthesis of adsorbents

UiO-66 and UiO-66-NH_2 had been successfully prepared with a modified solvothermal synthesis [27]. Typically, 0.317 g of $ZrCl_4$ and 0.226 g of H_2BDC were dissolved in 30 mL DMF followed by adding 2.5 mL acetic acid associated with ultrasound irradiation for 15 min. The obtained mixture was transferred into a Teflon-lined autoclave (volume: 100 mL) and heated in an electric oven at 120°C for 24 h. The same molar amount of NH_2-BDC was used to replace of H_2BDC for the synthesis of UiO-66-NH_2. The final product (denoted as UiO-66) was collected by centrifugation and then washed thoroughly using DMF, methanol, and deionized water. Finally, the MOFs was dried at 60°C for 24 h in a vacuum oven.

2.3. Characterization Methods

X-ray powder diffraction patterns (XRD) were recorded with an X-ray diffractometer (PANlytical, Netherlands). After evacuation for 12 h at 150°C, the surface areas and pore size of the adsorbents were measured by nitrogen adsorption at 77 K on a porosity analyzer (ASAP 2010 Micromeritics, USA). Fourier transform infrared (FTIR, Nicolet 6700, USA) was performed to confirm the functionalization of MOFs. Thermal gravimetric analysis (TGA) was conducted on a thermogravimetric analyzer (NETZSCH STA 409 PC/PG, Germany) under airflow at a heating rate of 10°C min^{-1} in the temperature range from 30°C to 800°C. liquid chromatograph (Waters e2695, USA) was used to detect solution concentration.

2.4. Adsorption experiments

2.4.1. General procedures for diflunisal adsorption

The stock solutions of diflunisal (50 mg L^{-1}) were prepared by dissolving diflunisal in methanol-water (30:70 v/v). A diflunisal calibration curve was obtained with a series of standard diflunisal solutions (10–50 mg L^{-1}) from stock solution by successive dilutions. The concentration of diflunisal was determined by liquid chromatograph and the calibration curve was used to determine the initial or equilibrium concentrations of diflunisal.

Before adsorption, the adsorbents were dried for 12 h at 100°C in vacuum conditions. The adsorbent (10.0 mg) was added to the diflunisal solution (50 mL, pH = 5) and the mixture was stirred with an incubated shaker for a fixed time (1–10 h) at 26°C and constant speed (160 rpm). After stirring the mixture, the adsorbents were separated from the solution by a polytetrafluoroethylene syringe filter (hydrophobic, 0.5 μm) and the residual diflunisal concentration was determined by liquid chromatograph. The adsorption results were analyzed with a pseudo-second-order nonlinear kinetic model [29] and Langmuir isotherm [30]. To calculate the amount of adsorbed diflunisal, the mass-balance relationship [Eq. (1)] was used:

$$q_t = \left(C_0 - C_t\right)\frac{V}{W} \tag{1}$$

where C_0 (mg/L) was the concentration at time 0, C_t (mg/L) was the concentration at time t, V (L) was the volume of the diflunisal solution, and W (g) was the weight of the adsorbents. To determine the effect of solution pH on diflunisal adsorption capacity, the solution pH was adjusted by adding 0.1 M solutions of HCl or NaOH. The regeneration of UiO-66-NH_2 was examined through desorption of the adsorbed diflunisal by ethanol treatment for 24 h and sonication for 30 min.

2.4.2. General procedures for salicylic acid and carbamazepine adsorption

The UiO-66, UiO-66-NH_2, and AC were used to adsorb salicylic acid and carbamazepine with a method that was similar to diflunisal adsorption. Salicylic acid and

carbamazepine solutions (50 mg L^{-1}) were obtained by dissolving in methanol water (30:70 v/v). After stirring for a fixed time (1–10 h), the residual concentrations of salicylic acid and carbamazepine were measured by liquid chromatograph. The calculation methods were similar to the diflunisal adsorption procedure.

3. Results and discussion

3.1. Characterization of the adsorbents

The XRD patterns of the materials could show crystal variation before and after the materials modified [29]. Thus, XRD was performed and the patterns of UiO-66, UiO-66-NH_2 Fig. 1a shows that the synthesized materials had the UiO-66 crystal structure because the patterns were identical to the simulated one (CCDC No. 889529). The nitrogen adsorption results in Fig. 1b reveals that the porosity of UiO-66-NH_2 slightly decreased compared with the UiO-66.

As shown in Table 1, This decrease in the porosity probably was responsible for the additional functional group of the organic moieties.

The FTIR spectra of UiO-66 and UiO-66-NH_2 are shown in Fig. 2a. A C–N stretching and sharp N–H wagging band were observed at 1,260 and 762 cm^{-1}, respectively, which indicates the existence of the NH_2 groups [30]. The TGA (Fig. 2b) shows that the thermal stabilities of the UiO-66s were slightly reduced due to the introduction of amino functional groups.

3.2. Adsorption results

3.2.1. Adsorption of diflunisal

Three adsorbents including UiO-66, UiO-66-NH_2, and AC were used for diflunisal adsorptions, respectively. The adsorption performances were tested for a contact period of 1–10 h. The solid lines in Fig. 3 describe the linear plots of the pseudo-second-order rate equations using the following Eq. (2):

$$\frac{t}{q_t} = \frac{1}{kq_e^2} + \frac{t}{q_e} \tag{2}$$

where q_t (mg/g) was the amount adsorbed at time t (h); q_e (mg/g) was the amount adsorbed at equilibrium obtained by linear changes of t/q_t with time t; k (g/mg h) was the pseudo-second-order rate constant.

The correlation parameters (R^2) in Table 2 exhibit that the adsorption data fit the pseudo-second-order model very well. Fig. 3 shows that the adsorption of diflunisal with UiO-66 and UiO-66-NH_2 was more effective than the AC. It suggested that the adsorption of diflunisal by UiO-66s was due to the presence of favorable interaction between the UiO-66s and diflunisal (as shown in 3.3. Adsorption mechanism). In addition, we found that the UiO-66-NH_2 had more rapid adsorption of diflunisal compared with the UiO-66. Therefore, besides a favorable interaction between UiO-66s and diflunisal, the acid-base interactions were also worthy of attention between the adsorbates and UiO-66-NH_2 even with a decreased pore size of UiO-66-NH_2.

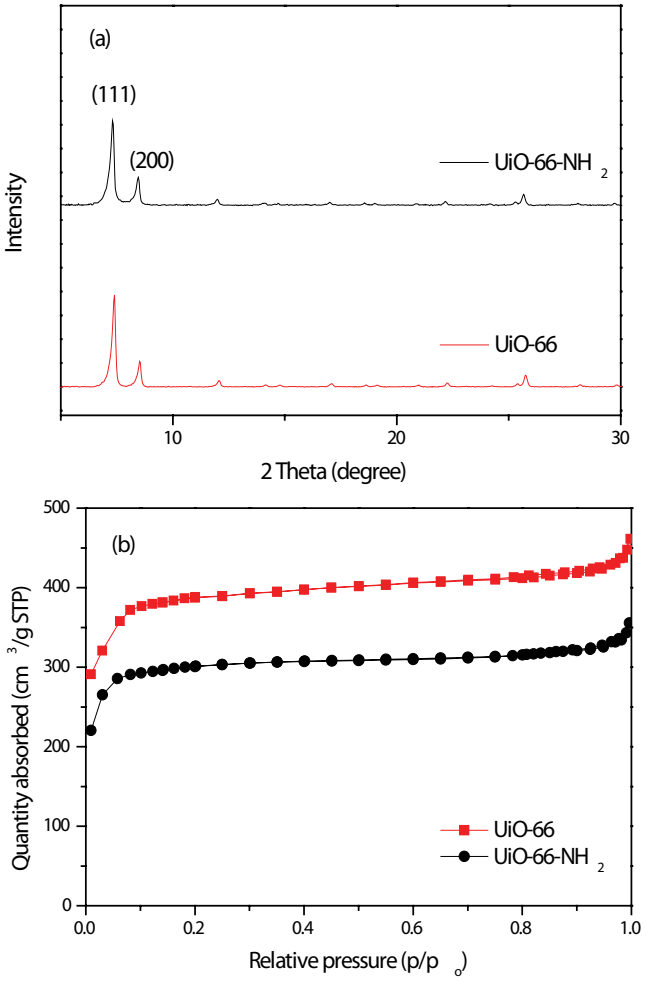

Fig. 1. (a) XRD patterns of the UiO-66s and (b) nitrogen adsorption isotherms.

Table 1
Textural properties of two adsorbents in this study

Adsorbents	SA_{BET} (m^2 g^{-1})	PV_{total} (cm^3 g^{-1})	$PV_{micropore}$ (cm^3 g^{-1})
UiO-66	1,561	0.55	0.49
UiO-66-NH_2	1,190	0.45	0.40
AC	1,387	0.51	0.46

AC: activated carbon.

The adsorption isotherms were obtained through occurring for the adsorption of diflunisal from a range of diflunisal concentrations (10–50 mg L^{-1}) for sufficient time of 10 h and they are shown in Fig. 4. Langmuir isotherm was used to exhibit the results and it was plotted according to the Langmuir equation [30]:

$$\frac{C_e}{q_e} = \frac{C_e}{Q_0} + \frac{1}{Q_0 b} \tag{3}$$

where C_e (mg/L) was the equilibrium concentration and Q_0 (mg/g) was the maximum adsorption capacity; b (L/mg) was the Langmuir constant and q_e (mg/g) was the amount adsorbed at equilibrium.

The Q_0 values were summarized in Table 2 and they showed that compared with the AC, the UiO-66s could adsorb a much higher amount of diflunisal. In addition, as shown in Table 2, UiO-66-NH_2 had a higher adsorption capacity than the virgin UiO-66. In most cases, the Q_0 value was determined by the pore volume and surface area of the adsorbents [30,31], but in the present study, the effects of functionalization were evident. The basic functionalized UiO-66 (with NH_2) led to acid-base interactions during the adsorption of diflunisal due to the acidity from the diflunisal. So functionalized adsorbents with basic NH_2 groups could increase the adsorption capacity of diflunisal in this study. A comparison between this work and previous data are presented in Table 3. It shows good adsorption capacity and wide-range use of UiO-66 and UiO-66-NH_2 in removing PPCPs.

3.2.2. *Adsorption of salicylic acid and carbamazepine*

The efficiencies of the studied adsorbents (virgin UiO-66, UiO-66-NH_2, and AC) in salicylic acid and carbamazepine adsorption were tested for a contact period of 1–10 h. The results are shown in Figs. 5a and b, respectively. The adsorption capability of salicylic acid was in the order: UiO-66-NH_2 > UiO-66 > AC. The reason for this could be explained that salicylic acid had a similar structure with

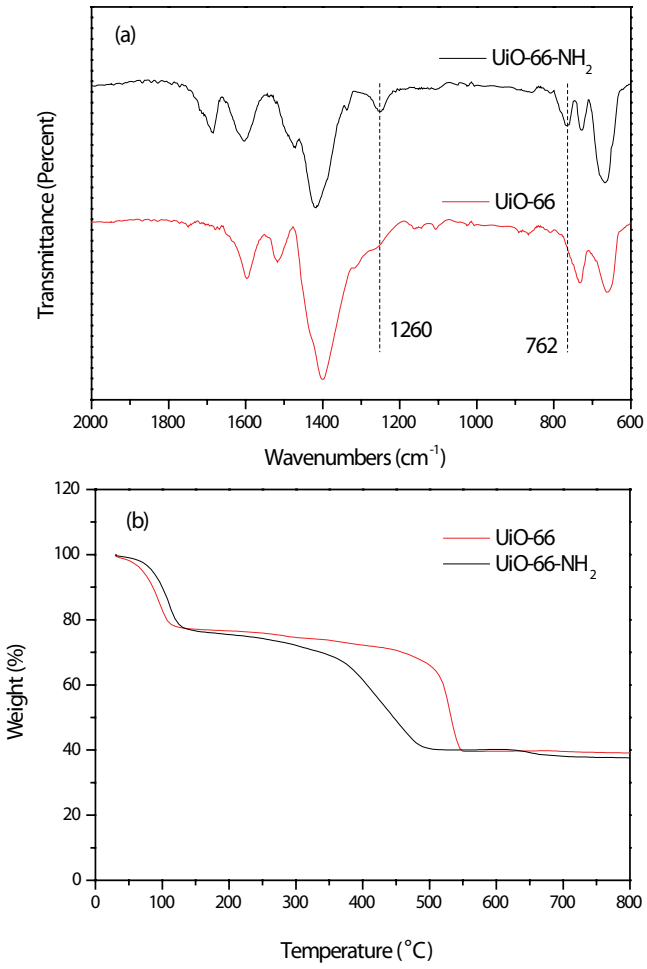

Fig. 2. (a) FTIR spectra and (b) TGA patterns of UiO-66s.

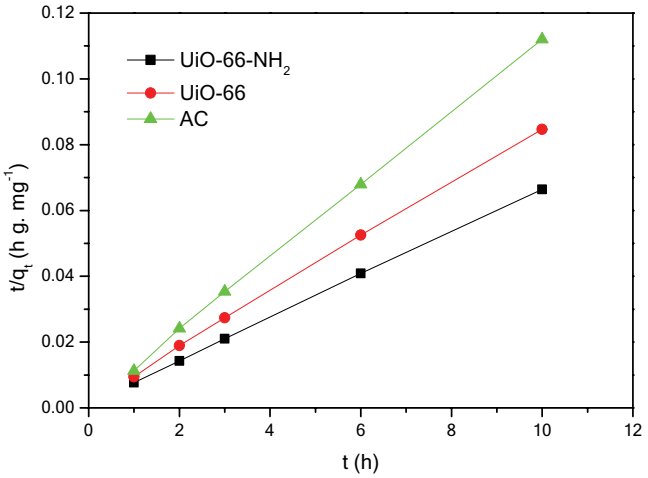

Fig. 3. Adsorption fit by the pseudo-second-order kinetics model of diflunisal over three adsorbents.

Table 2
Calculation results of the pseudo-second-order kinetic model and Langmuir isotherms with correlation coefficients (R^2) for adsorption of diflunisal over three adsorbents

Adsorbents	Pseudo-second-order kinetics		Langmuir isotherms	
	R^2	q_e (mg g^{-1})	R^2	q_0 (mg g^{-1})
UiO-66	0.996	116.1	0.997	109.5
UiO-66-NH_2	0.999	148.6	0.997	136.6
AC	0.997	88.5	0.994	83.3

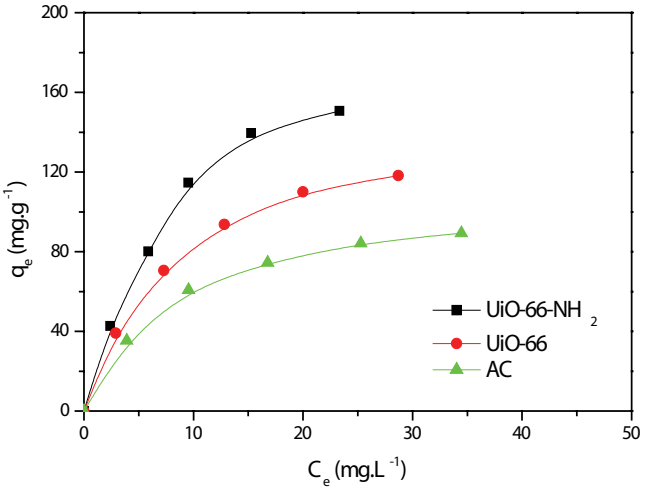

Fig. 4. Adsorption isotherms of diflunisal over the UiO-66s and AC at 26°C.

Table 3
A comparison between this work and previous data

Adsorbents	q_e (mg g^{-1})	PPCPs	References
UiO-66	58.5	Toluene	[32]
UiO-66	189	diclofenac	[36]
UiO-66	109.5	diflunisal	This work
UiO-66-NH$_2$	106	diclofenac	[36]
UiO-66-NH$_2$	136.6	diflunisal	This work

diflunisal. But the carbamazepine adsorption capability had a different tendency: UiO-66 > UiO-66-NH$_2$ > AC. The lower adsorption of carbamazepine by UiO-66-NH$_2$ compared with the virgin UiO-66 could be explained in terms of the Lewis base-base repulsion between the basic NH$_2$ groups of the UiO-66-NH$_2$ and the basic carbamazepine [33]. The adsorption isotherms of salicylic acid and carbamazepine are obtained in Fig. 6b and the results were consistent with the adsorption kinetics.

3.3. Adsorption mechanism

It was well-known that the Q_0 of porous adsorbent increased due to the increase of surface area. The nitrogen adsorption results in Fig. 1b reveals that the virgin UiO-66 had the highest BET surface area and Table 1 shows that all three adsorbents had sufficient total pore volume and micropore volume. At the same time, they all contained a certain amount of mesopores. Such a pore size distribution facilitated the mass transfer process of the adsorbed molecules from the surface of the adsorbent through the macropores to the mesopores to the micropores, and finally immobilized on the adsorbents [34]. Although UiO-66-NH$_2$ had less porosity than virgin UiO-66, it showed better adsorption performances for diflunisal and salicylic acid. It meant that the functional groups of the UiO-66-NH$_2$ increased the adsorption of diflunisal and salicylic acid. Conventional acid-base interaction was used to explain this phenomenon. However,

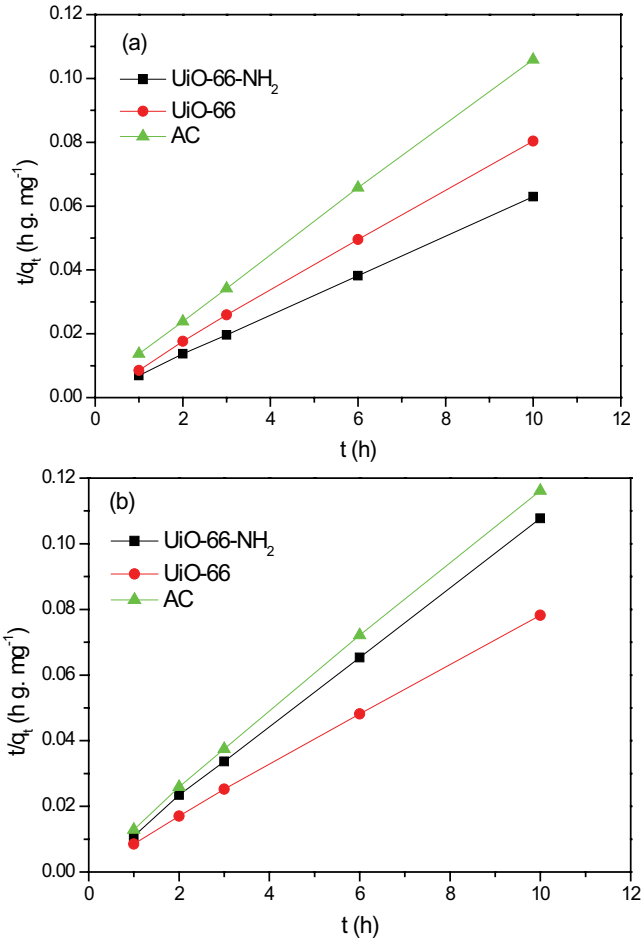

Fig. 5. Adsorption kinetics on (a) salicylic acid and (b) carbamazepine over the UiO-66s and AC.

the Q_0 of carbamazepine was reduced by the functionalization of UiO-66, which was due to the base–base repulsion between the NH$_2$ groups of the adsorbent and the NH$_2$ group of carbamazepine. π–π interaction between the benzene rings of UiO-66s and organic pollutants played a crucial role in adsorption [35].

Fig. 7 is used to describe the relationship between solution pH and the adsorption of diflunisal over UiO-66 [36]. The pKa of diflunisal was about 3.5 and the isoelectric point of UiO-66 was about 5.5. It meant that when the pH was >3.5, the adsorbate existed in a deprotonation form. In addition, the surface charge of UiO-66 maintained a positive value at a pH of ~5.5. Thus, electrostatic interactions between the diflunisal of deprotonation form and the UiO-66 with the positively charged surface, especially when the pH was <5.5, might be used to describe the advantageous adsorption of diflunisal. Fig. 7 shows that when solution pH was higher than 5.5, both diflunisal and the UiO-66 become negatively charged, which reduced the amount of diflunisal adsorption over the UiO-66. In addition, when the amount of neutral diflunisal molecules rising (pH < 3.5), the adsorption amount of diflunisal also decreased. Therefore, the adsorption of diflunisal decreased in the solution with both lower and higher pHs (Fig. 8).

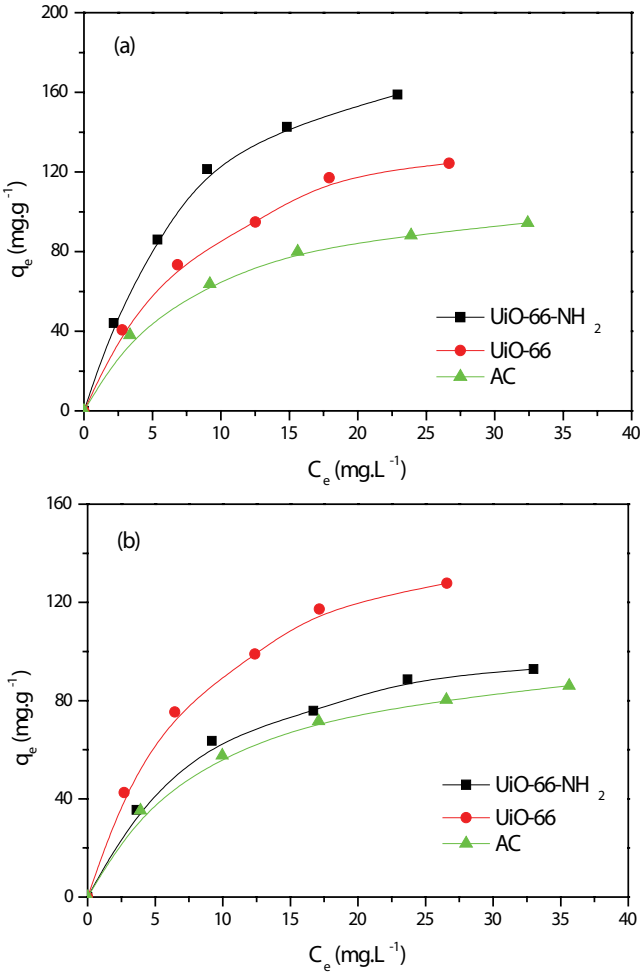

Fig. 6. Adsorption isotherms of (a) salicylic acid and (b) carbamazepine over the UiO-66s and AC at 26°C.

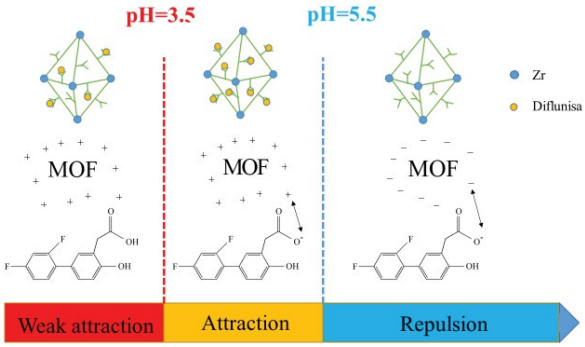

Fig. 7. The relationship between solution pH and the adsorption of diflunisal over UiO-66.

3.4. Reusability and competing ions

Reusability of adsorbents was considered as a crucial standard for applications. Therefore, in this study, the reusability of UiO-66-NH$_2$ was evaluated through washing regeneration by ethanol treatment for diflunisal. From Fig. 9 it can be concluded that the adsorption capacity of the

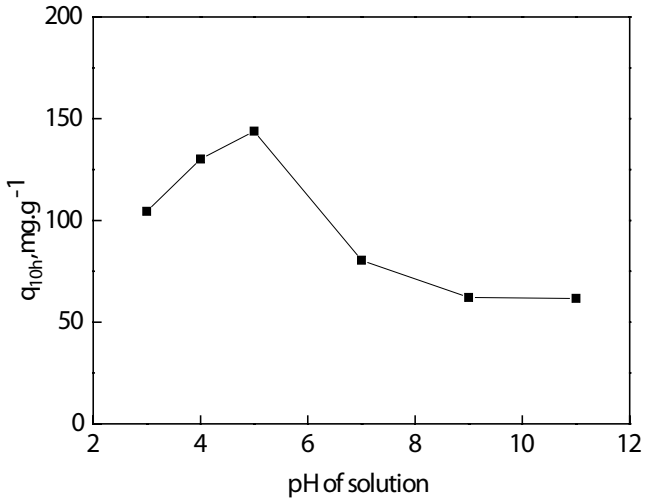

Fig. 8. Effect of solution pH on the adsorbed amounts of diflunisal over UiO-66 at 26°C.

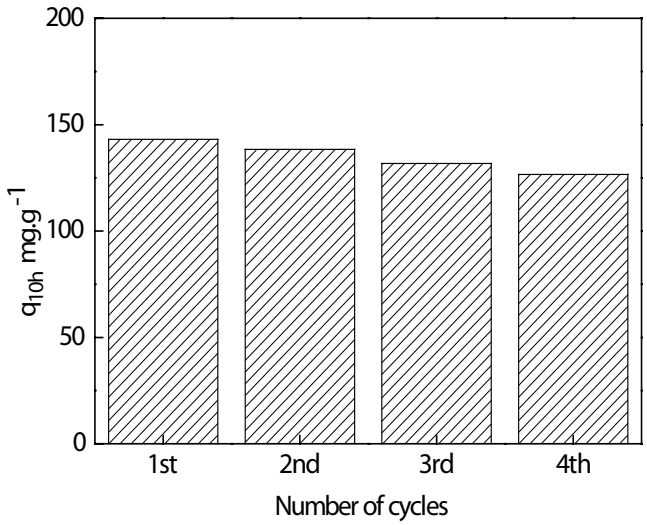

Fig. 9. Reusability of UiO-66-NH$_2$ for the adsorption of diflunisal after ethanol washing.

recycled UiO-66-NH$_2$ for diflunisal did not decrease obviously. Therefore, UiO-66-NH$_2$ can be used as a highly efficient regenerative adsorbent for the removal of diflunisal.

It is well-known that competing ions which exist in natural water can cause adsorption interference, which has an effect on the removal efficiency of the adsorbents, such as (Cl^-), (SO_4^{2-}), and (Na^+). Therefore, as shown in Fig. S1, when the concentration of (Cl^-) or (Na^+) reached 50 mg/L, the adsorption capacity of UiO-66-NH$_2$ hardly decreased and when (SO_4^{2-}) was present in water, the adsorption efficiency of UiO-66-NH$_2$ only decreased by 10%. Besides, the diflunisal adsorption efficiency over UiO-66 was almost unchanged even if common competing ions were present in the water. The experimental results showed that UiO-66-NH$_2$ and UiO-66 had good selectivity in the adsorption of diflunisal.

4. Conclusion

Virgin UiO-66 and UiO-66-NH_2 were applied in adsorption removal of PPCPs. The UiO-66s remarkably improved the adsorption of diflunisal, salicylic acid and carbamazepine compared with commercial AC. some specific interactions like π–π interaction (between the benzene rings of UiO-66s and organic pollutants) and electrostatic interactions (especially at pHs < 5.5) were used to explain the advantageous adsorption. Besides, UiO-66-NH_2 had a better performance in adsorption of diflunisal and salicylic acid than the virgin UiO-66, but the opposite trend was observed in adsorptive removal of carbamazepine. Favorable acid-base interactions and base-base repulsion between adsorbent and adsorbate could explain the adsorption performance, respectively. Finally, the UiO-66s could be regenerated by simply washing with ethanol. As a result, it could be viable to adsorptive removal of some PPCPs by using the UiO-66s.

Acknowledgments

The authors are grateful for the financial support provided by the Program for Changjiang Scholars and Innovative Research Team in University (IRT_17R97).

References

[1] B. Subedi, B. Du, C.K. Chambliss, J. Koschorreck, H. Rudel, M. Quack, B.W. Brooks, S. Usenko, Occurrence of pharmaceuticals and personal care products in German fish tissue: a national study, Environ. Sci. Technol., 46 (2012) 9047–9054.
[2] Q. Bu, B. Wang, J. Huang, S. Deng, G. Yu, Pharmaceuticals and personal care products in the aquatic environment in China: a review, J. Hazard. Mater., 262 (2013) 189–211.
[3] R. Feito, J.C.M. Rubio, J. Fernández, Occurrence of pharmaceuticals in river and tap waters of Toledo (Castilla-La Mancha Community, Spain), Toxicol. Lett., 196 (2010) S37–S351.
[4] W.A. Cabrera-Lafaurie, F.R. Roman, A.J. Hernandez-Maldonado, Transition metal modified and partially calcined inorganic-organic pillared clays for the adsorption of salicylic acid, clofibric acid, carbamazepine, and caffeine from water, J. Colloid. Interface Sci., 386 (2012) 381–391.
[5] A. Daneshvar, J. Svanfelt, L. Kronberg, G.A. Weyhenmeyer, Winter accumulation of acidic pharmaceuticals in a Swedish river, Enviro. Sci. Pollut. R, 17 (2010) 908–916.
[6] L. Joseph, J.R.V. Flora, Y.G. Park, M. Badawy, H. Saleh, Y. Yoon, Removal of natural organic matter from potential drinking water sources by combined coagulation and adsorption using carbon nanomaterials, Sep. Purif. Technol., 95 (2012) 64–72.
[7] J. Ryu, Y. Yoon, J. Oh, Occurrence of endocrine disrupting compounds and pharmaceuticals in 11 WWTPs in Seoul, Korea, J. Civ. Eng., 15 (2011) 57–64.
[8] J. Ryu, J. Oh, S.A. Snyder, Y. Yoon, Determination of micropollutants in combined sewer overflows and their removal in a wastewater treatment plant (Seoul, South Korea), Environ. Monit. Assess., 186 (2014) 3239–3251.
[9] K.H. Chu, Y.A.J. Al-Hamadani, C.M. Park, G. Lee, M. Jang, A. Jang, N. Her, A. Son, Y. Yoon, Ultrasonic treatment of endocrine disrupting compounds, pharmaceuticals, and personal care products in water: a review, Chem. Eng. J., 327 (2017) 629–647.
[10] X. Bian, Y. Xia, T. Zhan, L. Wang, W. Zhou, Q. Dai, J. Chen, Electrochemical removal of amoxicillin using a Cu doped PbO_2 electrode: electrode characterization, operational parameters optimization and degradation mechanism, Chemosphere, 233 (2019) 762–770.
[11] Q. Dai, J. Zhou, M. Weng, X. Luo, D. Feng, J. Chen, Electrochemical oxidation metronidazole with Co modified PbO_2 electrode: degradation and mechanism, Sep. Purif. Technol., 166 (2016) 109–116.
[12] Q. Dai, Y. Xia, C. Sun, M. Weng, J. Chen, J. Wang, J. Chen, Electrochemical degradation of levodopa with modified PbO_2 electrode: parameter optimization and degradation mechanism, Chem. Eng. J., 245 (2014) 359–366
[13] M. Weng, X. Yu, Electrochemical oxidation of para-aminophenol with rare earth doped lead dioxide electrodes: kinetics modeling and mechanism, Front. Chem., 7 (2019) 382.
[14] N.F.F. Moreira, C.A. Orge, A.R. Ribeiro, J.L. Faria, O.C. Nunes, M.F.R. Pereira, A.M.T. Silva, Fast mineralization and detoxification of amoxicillin and diclofenac by photocatalytic ozonation and application to an urban wastewater, Water. Res., 87 (2015) 87–96.
[15] Q. Dai, J. Wang, J. Yu, J. Chen, J. Chen, Catalytic ozonation for the degradation of acetylsalicylic acid in aqueous solution by magnetic CeO_2 nanometer catalyst particles, Appl. Catal., B, 144 (2014) 686–693.
[16] Q. Dai, W. Chen, J. Luo, X. Luo, Abatement kinetics of highly concentrated 1H-Benzotriazole in aqueous solution by ozonation, Sep. Purif. Technol., 183 (2017) 327–332.
[17] I. Ahmed, J.W. Jun, B.K. Jung, S.H. Jhung, Adsorptive denitrogenation of model fossil fuels with Lewis acid-loaded metal–organic frameworks (MOFs), Chem. Eng. J., 255 (2014) 623–629.
[18] C. Jung, J. Park, K.H. Lim, S. Park, J. Heo, N. Her, J. Oh, S. Yun, Y. Yoon, Adsorption of selected endocrine disrupting compounds and pharmaceuticals on activated biochars, J. Hazard. Mater., 263 (2013) 702–710.
[19] M. Weng, J. Pei, Electrochemical oxidation of reverse osmosis concentrate using a novel electrode: Parameter optimization and kinetics study, Desalination, 399 (2016) 21–28.
[20] Y. Hou, M. Qiu, M.G. Kim, P. Liu, G. Nam, T. Zhang, X. Zhuang, B. Yang, J. Cho, M. Chen, C. Yuan, L. Lei, X. Feng, Atomically dispersed nickel-nitrogen-sulfur species anchored on porous carbon nanosheets for efficient water oxidation, Nat. Commun., 10 (2019) 1392.
[21] P. Trens, H. Belarbi, C. Shepherd, P. Gonzalez, N.A. Ramsahye, U.H. Lee, Y.K. Seo, J.S. Chang, Adsorption and separation of xylene isomers vapors onto the chromium terephthalate-based porous material MIL-101(Cr): an experimental and computational study, Microporous Mesoporous Mater., 183 (2014) 17–22.
[22] J.L.C. Rowsell, O.M. Yaghi, Strategies for hydrogen storage in metal-organic frameworks, Angew. Chem. Int. Ed., 44 (2005) 4670–4679.
[23] E. Haque, J.W. Jun, S.H. Jhung, Adsorptive removal of methyl orange and methylene blue from aqueous solution with a metal-organic framework material, iron terephthalate (MOF-235), J. Hazard. Mater., 185 (2011) 507–511.
[24] E.V. Ramos-Fernandez, C. Pieters, B. Linden, J. Juan-Alcaniz, P. Serra-Crespo, M.W.G.M. Verhoeven, H. Niemantsverdriet, J. Gascon, F. Kapteijn, Highly dispersed platinum in metal-organic framework NH_2-MIL-101(Al) containing phosphotungstic acid – Characterization and catalytic performance, J. Catal., 289 (2012) 42–52.
[25] X. Li, Y. Liu, J. Wang, J. Gascon, J. Li, B. Bruggen, Metal-organic frameworks based membranes for liquid separation, Chem. Soc. Rev., 46 (2017) 7124–7144.
[26] A. Donnadio, R. Narducci, M. Casciola, F. Marmottini, R. D'Amato, M. Jazestani, H. Chiniforoshan, F. Costantino, Mixed Membrane Matrices (MMMs) based on Nafion/UiO-66/SO3H-UiO-66 Nano MOFs: revealing the effect of crystal size, sulfonation and filler loading on the mechanical and conductivity properties, ACS Appl. Mater. Interfaces, 9 (2017) 42239–42246.
[27] J.H. Cavka, S. Jakobsen, U. Olsbye, N. Guillou, C. Lamberti, S. Bordiga, K.P. Lillerud, A new zirconium inorganic building brick forming metal-organic frameworks with exceptional stability, J. Am. Chem. Soc., 130 (2008) 13850–13851.
[28] N. Yin, K. Wang, L. Wang, Z. Li, Amino-functionalized MOFs combining ceramic membrane ultrafiltration for Pb (II) removal, Chem. Eng. J., 306 (2016) 619–628.
[29] Y.J. Xia, X.Z. Bian, Y. Xia, W. Zhou, L. Wang, S.Q. Fan, P. Xiong, T.T. Zhan, Q.Z. Dai, J.M. Chen, Effect of indium doping on the

PbO_2 electrode for the enhanced electrochemical oxidation of aspirin: an electrode comparative study, Sep. Purif. Technol., 237 (2020) 116321.
[30] Z. Hasan, E.J. Choi, S.H. Jhung, Adsorption of naproxen and clofibric acid over a metal–organic framework MIL-101 functionalized with acidic and basic groups, Chem. Eng. J., 219 (2013) 537–544.
[31] H.R. Abid, H. Tian, H.M. Ang, M.O. Tade, C.E. Buckley, S. Wang, Nanosize Zr metal-organic framework (UiO-66) for hydrogen and carbon dioxide storage, Chem. Eng. J., 187 (2012) 415–420.
[32] R.N. Amador, L. Cirre, M. Carboni, D. Meyer, BTEX removal from aqueous solution with hydrophobic Zr metal-organic frameworks, J. Environ. Manage., 214 (2018) 17–22.
[33] I. Ahmed, S.H. Jhung, Effective adsorptive removal of indole from model fuel using a metal-organic framework functionalized with amino groups, J. Hazard. Mater., 283 (2015) 544–550.
[34] Y. Han, M. Liu, K. Li, Q. Sun, C. Song, G. Zhang, Z. Zhang, X. Guo, Cu_2O mediated synthesis of metal-organic framework UiO-66 in nanometer scale, Cryst. Growth Des., 17 (2017) 685–692.
[35] Z. Hasan, S.H. Jhung, Removal of hazardous organics from water using metal-organic frameworks (MOFs): plausible mechanisms for selective adsorptions, J. Hazard. Mater., 283 (2015) 329–339.
[36] Z. Hasan, N.A. Khan, S.H. Jhung, Adsorptive removal of diclofenac sodium from water with Zr-based metal–organic frameworks, Chem. Eng. J., 284 (2016) 1406–1413.

Supporting information

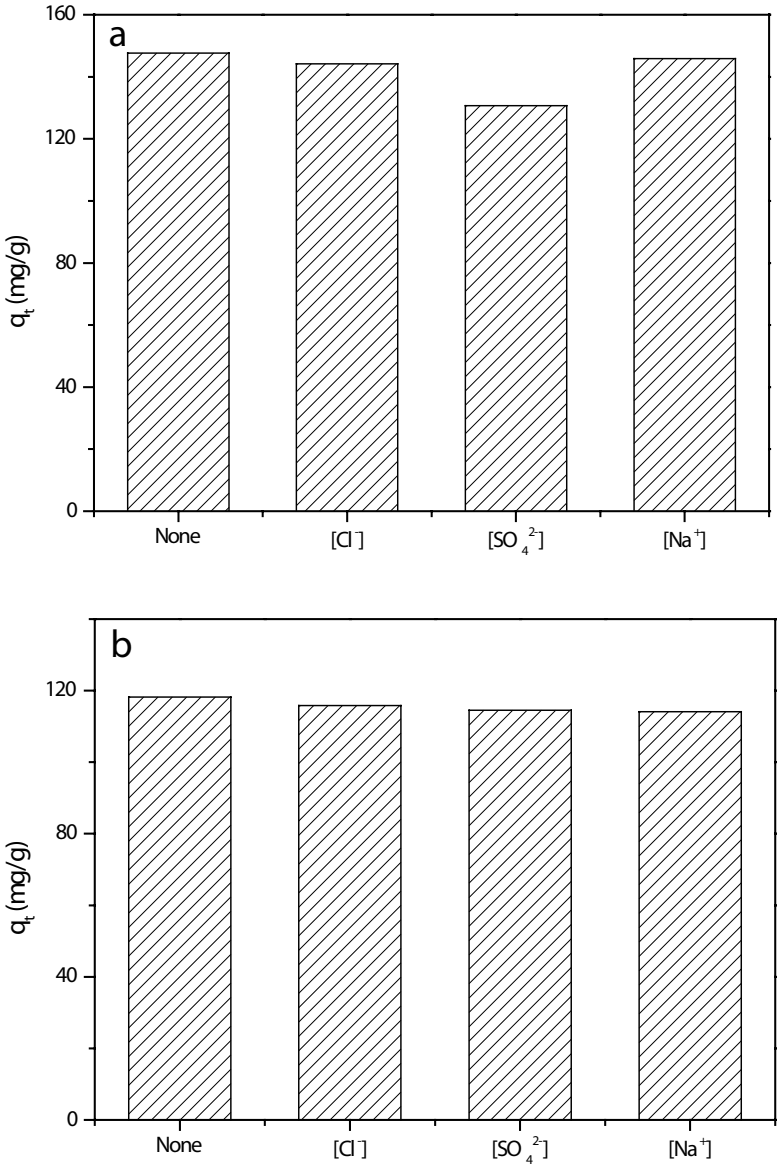

Fig. S1. Effects of competing ions on the adsorption of diflunisal over UiO-66-NH_2 (a) and UiO-66 (b). Conditions: adsorbent 10 mg; diflunisal solution 50 mL (50 mg/L); pH = 5; temperature 26°C; ion concentration 50 mg/L.